Author(s): Kumar, Parveen; Rautiainen, J. Mikko; Novotny, Jan; Ward, Jas S.; Marek, Radek; Rissanen, Kari; Puttreddy, Rakesh

Title: The impact of ortho-substituents on Bonding in Silver(I) and Halogen(I) complexes of 2-Mono- and 2,6-Disubstituted Pyridines : An In-depth Experimental and Theoretical Study

Year: 2024

Version: Published version

Chemistry–A European Journal
Research Article
doi.org/10.1002/chem.202303643
Chemistry Europe
European Chemical Societies Publishing
www.chemeurj.org

Hot Paper

The Impact of *ortho*-substituents on Bonding in Silver(I) and Halogen(I) Complexes of 2-Mono- and 2,6-Disubstituted Pyridines: An In-Depth Experimental and Theoretical Study

Parveen Kumar,[a] J. Mikko Rautiainen,[a] Jan Novotný,[b] Jas S. Ward,[a] Radek Marek,[b] Kari Rissanen,*[a] and Rakesh Puttreddy*[a]

The coordination nature of 2-mono- and 2,6-disubstituted pyridines with electron-withdrawing halogen and electron-donating methyl groups for $[N–X–N]^+$ (X = I, Br) complexations have been studied using ^{15}N NMR, X-ray crystallography, and Density Functional Theory (DFT) calculations. The ^{15}N NMR chemical shifts reveal iodine(I) and bromine(I) prefer to form complexes with 2-substituted pyridines and only 2,6-dimethylpyridine. The crystalline halogen(I) complexes of 2-substituted pyridines were characterized by using X-ray diffraction analysis, but 2,6-dihalopyridines were unable to form stable crystalline halogen(I) complexes due to the lower nucleophilicity of the pyridinic nitrogen. In contrast, the halogen(I) complexes of 2,6-dimethylpyridine, which has a more basic nitrogen, are characterized by X-crystallography, which complements the ^{15}N NMR studies. DFT calculations reveal that the bond energies for iodine(I) complexes vary between −291 and −351 kJ mol^{-1} and for bromine between −370 and −427 kJ mol^{-1}. The bond energies of halogen(I) complexes of 2-halopyridines with more nucleophilic nitrogen are 66-76 kJ mol^{-1} larger than those of analogous 2,6-dihalopyridines with less nucleophilic nitrogen. The experimental and DFT results show that the electronic influence of *ortho*-halogen substituents on pyridinic nitrogen leads to a completely different preference for the coordination bonding of halogen(I) ions, providing new insights into bonding in halogen(I) chemistry.

Introduction

[Bis(pyridine)halogen(I)]$^+$ complexes, $[Py–X–Py]^+$ (X = Cl, Br, I, Py = pyridine), are the extreme case of a halogen-bonded complex where the halogen atom has been fully ionized to cationic state X^+.[1] These complexes are typically prepared via a $[Py–Ag–Py]^+ \rightarrow [Py–X–Py]^+$ cation exchange method.[2] Their first synthesis was described in the 1930s by Carlshon,[3] and their iodine(I) crystal structure in the 1960s by Hassel *et al.*,[4] bromine(I) crystal structure by Robertson *et al.*,[5] chlorine(I) crystal structure by Riedel *et al.*,[6] and have been reviewed by Erdélyi *et al.*[1] and us.[7] Since the 1990s, these complexes have received a lot of attention as Barluenga's reagent in organic synthesis e.g., cyclizations,[8] iodinations,[9] and oxidations.[10] The binding of two identical pyridines to X^+ ion results in the formation of linear bis-coordinate homoleptic (or symmetrically ligated) complexes,[11] whereas two different pyridines give linear bis-coordinate heteroleptic (or asymmetrically ligated) complexes.[12] In comparison to the conventional homoleptic halogen(I) complexes, the scope and impact of heteroleptic complexes have been limited; yet their X^+ is chemically reactive, making them potentially valuable as halogenating reagents.

In their complexes, the $^+X–N(Py)$ bond belong to the class of halogen bonds (XBs),[13] a supramolecular interaction that is related to well-known hydrogen bonding (HB).[14] Because $^+X–N(Py)$ bonds of $[Py–X–Py]^+$ complexes have supramolecular covalency characteristics,[15] they have been used to prepare supramolecular capsules,[16] helicates,[17] and metal-organic frameworks.[18] Initially, the chemistry of halogen(I) complexes appeared simple, with halogen(I) adopting a $p_x^2p_y^2p_z^0$ arrangement and the two lobes of vacant p_z^0 accepting electron densities from pyridinic nitrogen for an $[N–X–N]^+$ XB interaction.[1] However, persistent research with a broad substrate scope resulted in fascinating discoveries. Examples include, (i) $[Py–I–Py]^+$ maintains symmetry both in polar aprotic solvents and crystals, and it is linear within experimental error.[11a,19] (ii) The $^+X–N$ bond lengths can be adjusted by substituents on pyridines, which has a direct impact not only on the bonding strengths but also opens up opportunities for symmetric and asymmetric $[N–X–N]^+$ motifs. For instance, a static asymmetric $[N–I\cdots N]^+$ bond geometry (two XBs of differ-

[a] Dr. P. Kumar, Dr. J. M. Rautiainen, Dr. J. S. Ward, Prof. Dr. K. Rissanen, Dr. R. Puttreddy
Department of chemistry
University of Jyvaskyla
Jyvaskyla, P.O. BOX 35, FI-40014 (Finland)
E-mail: kari.t.rissanen@jyu.fi
rakesh.r.puttreddy@jyu.fi
[b] Dr. J. Novotný, Prof. Dr. R. Marek
Department of Chemistry, Faculty of Science
Masaryk university
Kamenice 5, 62500 Brno (Czechia)

Supporting information for this article is available on the WWW under https://doi.org/10.1002/chem.202303643

ent strengths) was obtained in a [(1,2-bis(pyridin-2-ylethynyl)benzene)iodine(I)]$^+$ by adding a $-CH_3$ and a $-CF_3$ group at the *para*-position to the pyridinic-N, with the halogen residing closer to the nitrogen of higher electron density.[12a] (iii) The crystalline iodine(I) is nucleophilic and exhibits I···Ag interactions with Ag(I) cations.[20] Examples of these complexes include $[I(mtz)_2]$*$[Ag(bpy)_2](PF_6)_2$ and $[I(DMAP)_2]$*$[Ag(bpyMe_2)_2](PF_6)_2$ (*represents an I···Ag interaction). (iv) In the presence of two different pyridines with different nucleophilicities, iodine(I) exhibits a preference for complexation with the more nucleophilic pyridine.[21]

The plethora of discoveries in halogen(I) chemistry over the past few years improved our understanding of mechanisms and electronic structures and continues to provide new knowledge for ''isolobal'' cation exchange processes that use a wide range of *para*-substituted pyridines.[1,7,22] Contrarily, the halogen(I) chemistry of *ortho*-substituted pyridines is less known[11c] despite their evident importance in organic synthesis. For example, Wada *et al.* discovered that the iodocyclization of α-propargylic glycine derivatives yields pyrroles or 2,3-dihydropyrroles depending on the choice of iodine(I) reagents, $[Py–I–Py]^+$ and $[coll-I-coll]^+$ (Coll = 2,4,6-trimethylpyridine).[23] The use of $[Py–I–Py]^+$ exclusively gives 2,3-dihydropyrroles while the collidine-based reagent drives the cyclization to pyrroles. The former is attributed to symmetric $^+$I–N bond distances (2.259 Å) and near coplanarity of pyridyl rings (dihedral angle, θ = 1.2°) while the latter to the presence of asymmetric $^+$I–N bonds (2.272 and 2.304 Å) and twisted conformation of collidine rings (θ = 18.5°) caused by *ortho*-methyl groups about the $[N–I–N]^+$ motif. Another example by Rousseau *et al.*,[24] utilized the $[coll-I-coll]^+$ to perform a cyclic transformation on ω-alkenoic acids to produce iodomethyl-ω-caprolactones, which is not achievable with conventional iodine(I) reagents.

Herein, we investigate $[Py–X–Py]PF_6$ (X = I or Br) complexes formed by 2-mono- (**1**–**5**) and 2,6-disubstituted pyridines (**6**–**10**) to probe the coordination and structural properties of *ortho*-substituted pyridines by experimental and Density Functional Theory (DFT) studies (Scheme 1). Halogens are one of the many substitution types that attracted our interest since they offer a straightforward method to comprehend the pyridinic N-coordination for halogen electronegativity. The 2-methylpyridine (**5**) and 2,6-dimethylpyridine (**10**) comprising electron-donating methyl substituents will serve as a reference.

Results and Discussion

Solution NMR Studies

The $[L-Ag-L]^+$ silver(I) complexes are synthesised by mixing 2.0 eq of pyridines (**L** = **1**-**10**) with 1.0 eq silver(I) salts in acetone-d_6 (For details, see ESI). ^{1}H and ^{15}N NMR spectroscopy were used to monitor the conversion of the free pyridine ligand to the silver(I) complex. The $[L–X–L]^+$ (X = I or Br) complexes were then synthesized via the $[L–Ag–L]^+ \rightarrow [L–X–L]^+$ cation exchange reaction by adding 1.1 eq of iodine or bromine to a solution containing silver(I) complex, resulting in the precipitation of silver halide.[11a] The silver halide solids were removed by filtration, and the filtrate was used for NMR studies (For details, see Figures S1-S56). Ligands as their trifluoroacetate (TFA) salts were prepared for NMR studies to determine whether $[LH]^+$ is present in the $[L–Ag–L]^+ \rightarrow [L–X–L]^+$ cation exchange reactions.

The decrease in the paramagnetic deshielding term on pyridinic nitrogen upon metal complexation due to the replacement of n-π* electron transitions by σ-π* transitions[25] has been used to explain lower nitrogen chemical shifts of nitrogen-metal complexes compared to their non-coordinated state. On this premise, the coordination shift $\Delta\delta(^{15}N)$, defined as the difference in $\delta(^{15}N)$ chemical shift between a complex and its corresponding pyridine ligand, has been widely used for measuring the interaction strengths of metal[26] and halogen(I)[27] complexes. Thus, the ^{15}N NMR of silver(I), halogen(I) and HB complexes are acquired in acetone-d_6 at −10 °C. The δ^{15}N of free pyridines and

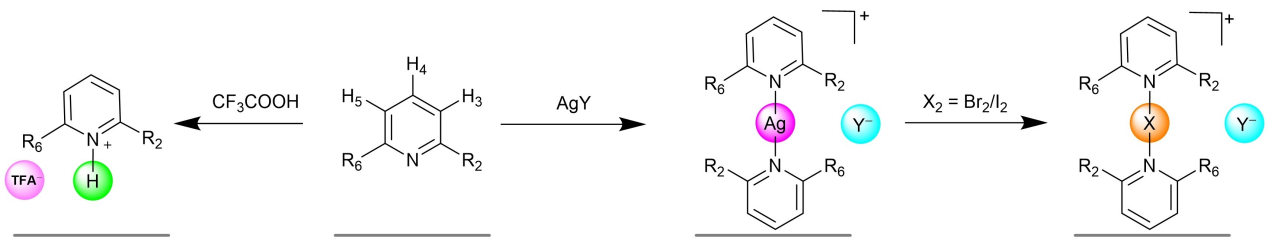

[**1**H]TFA
[**2**H]TFA
[**3**H]TFA
[**4**H]TFA
[**5**H]TFA
[**6**H]TFA
[**7**H]TFA
[**8**H]TFA
[**9**H]TFA
[**10**H]TFA

(**1**) R_2 = F, R_6 = H
(**2**) R_2 = Cl, R_6 = H
(**3**) R_2 = Br, R_6 = H
(**4**) R_2 = I, R_6 = H
(**5**) R_2 = CH_3, R_6 = H
(**6**) R_2,R_6 = F
(**7**) R_2,R_6 = Cl
(**8**) R_2,R_6 = Br
(**9**) R_2,R_6 = I
(**10**) R_2,R_6 = CH_3

[**1**–Ag–**1**]Y
[**2**–Ag–**2**]Y
[**3**–Ag–**3**]Y
[**4**–Ag–**4**]Y
[**5**–Ag–**5**]Y
[**6**–Ag–**6**]Y
[**7**–Ag–**7**]Y
[**8**–Ag–**8**]Y
[**9**–Ag–**9**]Y
[**10**–Ag–**10**]Y

[**1**–X–**1**]Y
[**2**–X–**2**]Y
[**3**–X–**3**]Y
[**4**–X–**4**]Y
[**5**–X–**5**]Y
[**6**–X–**6**]Y
[**7**–X–**7**]Y
[**8**–X–**8**]Y
[**9**–X–**9**]Y
[**10**–X–**10**]Y

Scheme 1. Chemical structures and general synthesis route to prepare [**L**-Ag-**L**]Y (Y = PF_6), [**L**-X-**L**]Y (X = I, Br; Y = PF_6), [LH]TFA complexes of 2-substituted pyridines (**1**-**5**) and 2,6-disubstituted pyridines (**6**-**10**).

the $\Delta\delta(^{15}N)$ values of their complexes are given in Table 1. The ^{1}H NMR data is included in the Supporting Information (Table S1).

The $\delta(^{15}N)$ values of free halopyridines indicate a larger shielding as the halogen electronegativity increases, with the largest ^{15}N chemical shifts observed for **1** and **6** with fluorine substituents. This results from the reduced paramagnetic deshielding linked to the nitrogen non-bonding orbital (n-π* transitions, see above). We thus predicted the halopyridinic nitrogen coordination power, or $\Delta\delta(^{15}N)$ values, would follow the reverse order i.e., **4** > **3** > **2** > **1** and **9** > **8** > **7** > **6**. However, the $\Delta\delta(^{15}N)$ values of 2-chloro-, 2-bromo-, and 2-iodopyridine-Ag(I) complexes are nearly the same, with a maximum difference of 1–2 ppm. The $\Delta\delta(^{15}N)$ values of 2-halopyridine-I(I) and -Br(I) complexes show random trends, **4** > **2** > **3** > **1** and **3** > **4** > **2** > **1**, respectively. The $\Delta\delta(^{15}N)$ values of 2-halopyridine-Ag(I), -I(I) and -Br(I) are 22–25, 40–81, and 15–43 ppm smaller in comparison to the analogous 2-methylpyridine complexes. This suggests the 2-halopyridinic-N is less nucleophilic owing to the electron-withdrawing property of the halogen substituents, and as a result, weaker coordination power to silver and halogen cations.

The $\Delta\delta(^{15}N)$ values of the 2,6-dihalopyridine-Ag(I)/X(I) are significantly smaller than those of analogous 2-halopyridine-Ag(I)/X(I) complexes, which range from −2.5 to −7.6 ppm for silver(I), −0.6 to −9.3 ppm for iodine(I), and −0.2 to −16.6 ppm for bromine(I). Smaller $\Delta\delta(^{15}N)$ values of 2,6-dihalopyridine complexes can be attributed to the presence of two electron-withdrawing *ortho*-halogens adjacent to the pyridinic-N thus weakening the coordination power of nitrogen. The $\Delta\delta(^{15}N)$ values of 2,6-dihalopyridine-Ag(I) complexes show a random trend, **9** > **7** > **8** > **6**, and there is no opportunity to establish trends for 2,6-dihalopyridine-I(I)/Br(I) complexes since [**6**-X-**6**]$^+$, [**7**-X-**7**]$^+$, and [**8**-X-**8**]$^+$ all fall within the experimental error range (1-2 ppm). Note that the $\delta^{15}N$ values of 2-bromopyridine (**3**) with electron-withdrawing bromine and of 2-methylpyridine (**5**) with electron-donating methyl are the same (Table 1). But the $\Delta\delta^{15}N$ values of **3** in silver(I), iodine(I), and bromine(I) are 25, 53, and 15 ppm smaller than in the comparable complexes formed by **5**. Similarly, the $\delta^{15}N$ of 2,6-dibromopyridine (**8**) and 2,6-dimethylpyridine (**10**) are the same, but $\Delta\delta^{15}N$ values of **8** in their silver(I), iodine(I), and bromine(I) are 45.6, 35.3, and 62.6 ppm smaller than in the analogous complexes formed by **10**.

Table 1. ^{15}N NMR chemical shifts (δ in ppm) of **1–10** and their $\Delta\delta(^{15}N)$ values[+] ($=\delta^{15}N_{compl}-\delta^{15}N_{lig}$) of silver(I), halogen(I) and hydrogen bond complexes in acetone-d_6

L	$\delta(^{15}N_{lig})$	$\Delta\delta(^{15}N_{Ag})$	$\Delta\delta(^{15}N_{I})$	$\Delta\delta(^{15}N_{Br})$	$\Delta\delta(^{15}N_{H})$
1	−104.2	−27.2	−21.2	−33.7	−0.2
2	−69.7	−31	−55.3	−39.0	−2.4
3	−61.5*	−28	−48.7	−62.0[†]	−1.7
4	−45.3*	−29.2	−65.3	−56.0[†]	−5.7
5	−61.7	−52.7	−102.0	−77.0	−100.6
6	−133.8	−2.5	−0.6	−0.2	−0.2
7	−77.5	−6.7	−1.0	−0.9	−0.8
8	−62.6	−4.4	−1.7	−0.8	−0.5
9	−34.6	−7.6	−9.3	−16.6	−1.2
10	−62.2	−49.8	−90	−69.4	−101.9

[+] Note that sovlents effects can have a substantial impact on the N-coordination of solvated free pyridines. As a result, similar $\Delta\delta(^{15}N)$ may result from the compensation of two effects, i.e., different desolvation and complexation mechanisms. [†]Their ^{15}N NMR data was collected at −20 °C since no signals were observed at −10 °C.* The $\delta(^{15}N)$ values of **3** (−61.6 ppm) and **4** (−45.3 ppm) at −20 °C are equal to those at −10 °C.

The $\Delta\delta(^{15}N)$ of 2-halopyridine-H complexes varies between 0 and −5.7 ppm, whereas that of 2-methylpyridine-H is −101 ppm suggesting 2-halopyridines are forming (TFA)O–H···N_{Py} type HB complexes, while the 2-methylpyridine is forming (TFA)O$^-$···[HNPy]$^+$ salt owing to the more nucleophilic nitrogen of 2-methylpyridine. It is noteworthy that the $\Delta\delta(^{15}N)$ values of 2-halopyridine-H complexes are very different from those of its 2-halopyridine-X(I), thus establishing the existence of halogen(I) species. Among the 2,6-disubstituted pyridines, the $\Delta\delta(^{15}N)$ values of 2,6-dihalopyridine-H complexes are practically 0 ppm, whereas the 2,6-dimethylpyridine-H has a value of −102 ppm. The existence of 2,6-dihalopyridine-X(I) species, except for 2,6-diiodo- and 2,6-dimethylpyridine-X(I), casts doubt since their $\Delta\delta(^{15}N)$ values are nearly the same as those of 2,6-dihalopyridine-H complexes. The 2,6-diiodo- and 2,6-dimethylpyridine-X(I) and their H-complexes have distinct $\Delta\delta(^{15}N)$ values, supporting the formation of their halogen(I) complexes. This may account for why 2,6-dihalopyridines fail to produce halogen(I) crystal structures while 2,6-dimethylpyridine is successful (See Table 2). Similarly to 2-substituted pyridine H-complexes, the $\Delta\delta(^{15}N)$ values of 2,6-dihalopyridines are forming (TFA)O–H···N_{Py} type HB complexes, and the 2,6-dimethylpyridine is forming a (TFA)O$^-$···[HNPy]$^+$ HB salt. The electron-poor nitrogen in 2,6-dihalopyridines and the electron-rich nitrogen in 2,6-dimethylpyridine are the fundamental reason for these very distinct $\Delta\delta(^{15}N)$ values.

Inspired by large differences in the $\Delta\delta(^{15}N)$ values of 2,6-disubstituted pyridine-X(I) complexes, ligand-exchange reactions were carried out on [**9**-Ag-**9**]$^+$ using **10** as shown in Figure 1. The ^{1}H NMR spectra of [**9**-Ag-**9**]$^+$ shows single set of aromatic protons for **9** (Figure 1b), and its chemical shifts differ from those of pure **9** (Figure 1a), suggesting the formation of a silver(I) complex. Upon addition of free **10** (the strongest XB acceptor in the 2,6-substituted pyridine series) to [**9**-Ag-**9**]$^+$, weakly coordinating **9** is replaced by **10** (blue signals), yielding [**10**-Ag-**10**]$^+$. Upon the addition of elemental iodine (1.1 eq) to this mixture, the [**10**-Ag-**10**]$^+$ undergoes a cation exchange reaction resulting in [**10**-I-**10**]$^+$ species. Note that the physical form of **9** is a white solid and **10** is a colourless liquid. Ligand **9** crashes out as solid from the solution upon the addition of **10**, and in the mixture, there is some free **9**, whose chemical shifts match the pure **9**, that does not participate in $^+$Ag–N (Figure 1c) and $^+$I–N bonding (Figure 1d). The $\delta(^{15}N)$ and $\Delta\delta(^{15}N)$ values of **9**, **9** in [**9**-Ag-**9**]PF_6, **9** and **10** in [**10**-Ag-**10**]PF_6 + **9**, as well as **9** and **10** in [**10**-I-**10**]PF_6 + **9** + AgI are the same as those listed in Table 1. Similar results were obtained when ligand exchange was performed on [**L**-Ag-**L**]$^+$ (**L** = **7**,**8**) by using **10** (For

Table 2. Selected bond parameters in crystal structures of silver(I), iodine(I) and bromine(I) complexes.

Code	d(Ag–N) Å d(N···N')Å, θ (°)	∠N–Ag-N (°)	Code	d(I–N) Å d(N···N')Å, θ (°)	∠N–I–N (°)	Code	d(Br–N) Å d(N···N')Å, θ (°)	∠N–Br–N (°)
[**1**-Ag-**1**]PF_6	–*	–*	[**1**-I-**1**]PF_6	2.263(2) 4.55, 38.2	175.69(8)	[**1**-Br-**1**]PF_6	2.098(4) 4.20, 38.8	176.3(2)
[**2**-Ag-**2**]PF_6	2.150(4) 4.30, 0	178.05(19)	[**2**-I-**2**]PF_6	–*	–*	[**2**-Br-**2**]PF_6	–*	–*
[**2**-Ag-**2**]Otf	2.210(3), 2.224(3) 4.35, 60.3	157.69(10)	[**2**-I-**2**]Otf	–*	–*	[**2**-Br-**2**]Otf	–*	–*
[**3**-Ag-**3**]PF_6	2.151(4), 2.150(4) 4.30, 32.2	176.01(13)	[**3**-I-**3**]PF_6	2.265(3), 2.288(4), 4.55, 52.1 2.265(3), 4.53, 0	176.86(12) 180.0	[**3**-Br-**3**]PF_6	2.097(3) 4.19, 0	177.23(15)
[**4**-Ag-**4**]PF_6	2.162(3), 2.161(3) 4.32, 43.0	176.51(11)	[**4**-I-**4**]PF_6	2.262(2), 2.298(2) 4.56, 10.4	176.99(9)	[**4**-Br-**4**]PF_6	2.094(5), 2.113(5) 4.21, 16.7 2.081(2), 4.14, 7.3	175.6(2) 169.5(2)
[**5**-Ag-**5**]PF_6	2.124(2), 2.125(2) 4.25, 4.8	178.31(7)	[**5**-I-**5**]PF_6	2.262(7) 4.52, 0	180.0	[**5**-Br-**5**]PF_6	2.095(2) 4.19, 0	180.0
–*	–*	–*	–*	–*	–*	[**5**-Br-**5**]Br_3	2.095(5) 4.19, 0	180.0
[**6**-Ag-**6**]PF_6	–*	–*	[**6**-I-**6**]PF_6	–*	–*	[**6**-Br-**6**]PF_6	–*	–*
[**7**-Ag-**7**]Otf	2.210(3), 2.217(3) 4.42, 41.2	174.74(12)	[**7**-I-**7**]BF_4	–*	–*	[**7**-Br-**7**]BF_4	–*	–*
[**8**-Ag-**8**]BF_4	2.170(3) 4.34, 44.1	178.97(16)	[**8**-I-**8**]BF_4	–*	–*	[**8**-Br-**8**]BF_4	–*	–*
[**8**-Ag-**8**]Otf	2.223(4), 2.210(4) 4.42, 46.0	171.39(14)	[**8**-I-**8**] Otf	–*	–*	[**8**-Br-**8**]Otf	–*	–*
[**9**-Ag-**9**]PF_6	2.218(5), 2.207(5) 4.42, 43.1	176.2(2)	[**9**-I-**9**]PF_6	–*	–*	[**9**-Br-**9**]PF_6	–*	–*
[**9**-Ag-**9**]Otf	2.248(7), 2.246(7) 4.48, 47.6	171.2(3)	[**9**-I-**9**]Otf	–*	–*	[**9**-Br-**9**]Otf	–*	–*
[**10**-Ag-**10**]PF_6	2.139(3) 4.28, 51.2	178.86(13)	[**10**-I-**10**]PF_6	2.293(12) 4.59, 0	180.0	[**10**-Br-**10**]PF_6	2.120(4) 4.24, 0	180.0
[**10**-Ag-**10**]Otf	2.153(2), 2.152(2) 4.30, 11.4	173.63(6)	[**10**-I-**10**]Otf	–*		[**10**-Br-**10**]Otf	2.080(11), 2.173(10) 4.25, 17.1	178.3(4)
–*	–*	–*	–*	–*		[**10**-Br-**10**]Br_3	2.121(4) 4.24, 0	180.0

*X-ray crystal structure not available.

details, see Figures S12-S13). The viability of the ligand exchange process appears to be substantially influenced by the difference in Lewis basicities between the two ligands involved, and analogous ligand exchange instances in iodine(I) complexes, even though iodine(I) is a reactive entity, parallel the Erdélyi *et al.*[21] and our study.[12b]

X-ray Crystallography

Twenty-five crystal structures were examined to understand the bond properties and the structural arrangements of [**L**-Ag-**L**]$^+$ and [**L**–X-**L**]$^+$complexes (Figures S57-S81). The crystal structures of 12 silver(I) and 13 halogen(I) complexes can be divided into three classes: 1) asymmetric units with a "full" 2:1 ligand-to-silver(I)/halogen(I) ratio complex, 2) asymmetric units with the silver(I)/halogen(I) ion on a crystallographic inversion centre, and 3) asymmetric units with a combination of full 2:1 ligand-to-silver(I)/halogen(I) and centrosymmetric 2:1 structures. Overall, 11/25 complexes fall into class I, 12/25 into class II, and 2/25 into class III. Among the 13 halogen(I) complexes, 2/13 are class I, 9/13 are class II, and 2/13 are class III. A CSD search on halogen(I) complexes revealed a total of 88 hits, of which 26/88 belong to class I, 32/88 to class II, and 13/88 to class III. The

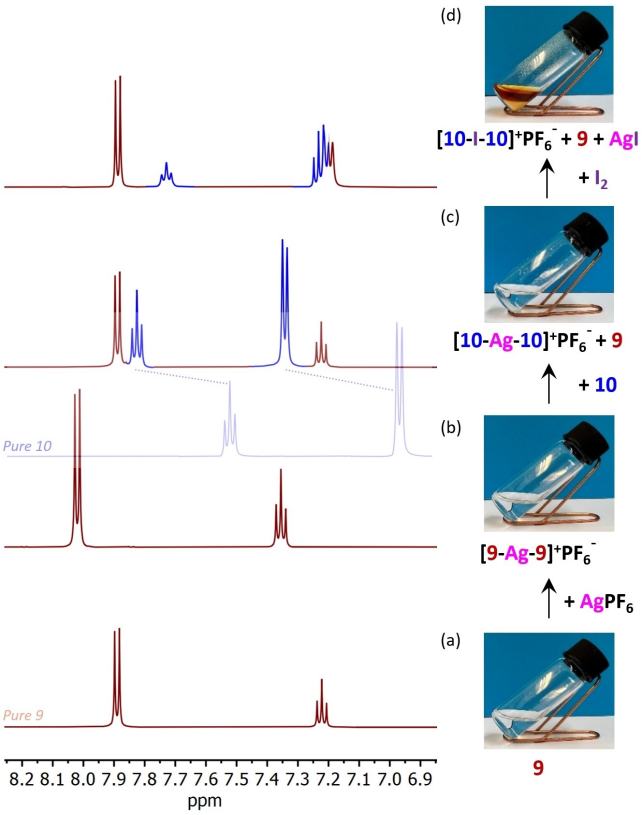

Figure 1. ^{1}H NMR stack spectra of ligand exchange studies using **9** and **10** in acetone-d_6 (500 MHZ, 298 K). Maroon colour ^{1}H corresponds to **9** and blue signals to **10**. The light blue colour ^{1}H NMR spectra above the ^{1}H NMR spectra of [**9**-Ag-**9**]$^{+}$ corresponds to the pure **10**.

remaining 17/88 are either disordered, do not have 3-D coordinates, or are co-crystallized with a 2:1 pyridine:Ag(I) complexes. This analysis demonstrates that crystalline halogen(I) complexes exhibit a strong preference for centrosymmetric class II and III complexes, with any deviation from this preference, such as class I, being potentially attributed to packing forces. Note that the outcome of silver(I) complexes is highly dependent on the pyridines used, the solvent, the anion, and packing interactions.[27a] These factors should be taken into account when examining the properties and behaviour of silver(I) complexes.

The $^{+}$Ag–N distances vary from 2.124(2) to 2.247(7) Å, $^{+}$I–N from 2.261 - 2.297(2) Å and $^{+}$Br–N from 2.080(11) to 2.173(10) Å. The difference between N–Ag/X^{+} and $^{+}$X/Ag–N′ distances is small for classes I and -III comprising two different bond distances and is in the range of 0.001–0.014 Å range for $^{+}$Ag–N, 0.023–0.036 Å for $^{+}$I–N and 0.019–0.093 Å for $^{+}$Br–N.

The N···N′ distances systematically increase as the ion radii increase in the order Br < Ag < I. Note the N···N′ distances in 2-halopyridine-Ag(I) complexes are 0.10–0.18 Å longer than those in analogous 2,6-dihalopyridine-Ag(I), systematically increase as the ion radii increase in the order Br < Ag < I. Note that N···N′ distances in 2-halopyridine-Ag(I) complexes (for the same anion) are 0.10 to 0.18 Å longer than those in analogous 2,6-dihalopyridine-Ag(I). This suggests that 2,6-dihalogens lower the electron density of their pyridinic-N and weakens its coordination to silver(I), which results in (i) longer N···N′ distances, and (ii) a lower degree of charge delocalization into pyridines, and consequently, a higher atomic charge on silver(I) (see Table 3).[27a] The class II complexes are more linear [177.26(17)–180°] compared to classes I and -III [157.69(10)–178.3(4)°], and angles are comparable to reported [bis(pyridine)Ag/X]$^{+}$ complexes.[28] The N–Ag/Br–N angles of [**2**-Ag-**2**]Otf and [**4**-Br-**4**]PF$_6$ deviate significantly from linearity, 157.69(10) and 169.5(2)°, respectively. The larger deviation in the silver complex is due to triflate anion coordination to silver(I) [d(O···Ag) = 2.618(3) Å], and its four-coordinate silver(I) is a seesaw geometry (τ_4 = 0.76),[29] while the deviation in bromine(I) complex likely originates from the crystal packing forces. Note that the [**4**-Br-**4**]PF$_6$ (175.6(2)°) has the largest deviation of the linear geometry of bromine(I) complexes ever observed, while the [**1**-Br-**1**]PF$_6$ (175.69(8)°) is close to the largest deviation of the geometry of helicate iodine(I) complex (174.2(2)° CCDC code: NOMBUP)[17] reported in the literature. Nonetheless, the overall N–Ag/X–N motifs are essentially linear when the minor $^{+}$Ag/$^{+}$X–N bond variations are considered as packing forces.

Ortho-substituent electronic effects only slightly affect the solid-state $^{+}$Ag/X–N distances. For example, the comparable $^{+}$X–N distances in [**2**-X-**2**]$^{+}$ (X = I, 2.263(2) Å; X = Br, 2,098(4) Å) of less nucleophilic 2-fluoropyridine and [**5**-X-**5**]$^{+}$ (X = I, 2.262(7) Å; X = Br, 2.095(2) Å) of more nucleophilic 2-methylpyridine suggest not only a tight overlapping between pyridine N-atom lone pair and halogen σ-hole as well as a stronger π-electron delocalization across [N–X–N]$^{+}$ bonds.[11a] This phenomenon, which is independent of the electron density of the 2-substituted pyridinic-N, suggests that bond lengths should be carefully related to the substituent's electron-directing effects.

The two pyridine rings across the N–X–N bonds are not coplanar, the interplanar angles between two pyridines, defined as θ (Figure 2d), are larger in silver(I) complexes (0–64.0°) and smaller for iodine(I) (0–52.1°) and bromine(I) (0–38.3°). Similar angles for halogen(I) complexes have been reported in the literature, suggesting that θ > 0° scenarios are not due to steric hindrance between the *ortho*-substituents across the N–Ag/X–N motifs but can be attributed to the crystal packing forces. However, it should be noted that the pyridine rings with bulky *ortho*-substituents may assume a θ > 0° arrangement about the N–X–N motif when N···N distances are e.g., < 3.0 Å to avoid steric conflict between the substituents. This situation has not yet been systematically investigated in X-ray crystal structures. In the X-ray crystal structure of [**2**-H···**2**]PF$_6$, the aromatic rings are genuinely forming a *trans*-conformation across the $^{+}$N–H···N motif to avoid the steric clash between the chlorine substituents and their N···N distance is 2.76 Å (See Figure S82).

Crystal packing analysis revealed several weak yet significant interactions between [Py–X–Py]$^{+}$ skeletons and counter anions, such as π/Br/I···F(anion). In particular, the iodine substituents of [**4**-I-**4**]$^{+}$ and the fluorine in the PF$_6$ form a C–I···F interactions (3.30 and 3.32 Å), and this structure is similar to Beer's pincer-type bis-iodotriazole pyridinium cationic receptor[30] for halide anions recognition by halogen bonds

Table 3. Halogen-bond interaction energies ΔE_{XB} (kJ mol^{-1})[*] calculated at M06-2X/def2-TZVP level of theory and QTAIM atomic charges of Ag^+, I^+ and Br^+ ions in their silver(I) and iodine(I) and bromine(I) complexes.

	Silver(I)				Iodine(I)				Bromine(I)			
Code	N	C2/C6	N	C2/C6	Ag	$\Delta E_{XB}^{\#}$	N	C2/C6	I	ΔE_{XB}	N	C2/C6	Br	ΔE_{XB}
1	−1.23	+1.19/+0.54	−1.28	+1.16/+0.51	+0.68	−190	−1.30	+1.18/+0.50	+0.56	−317	−1.23	+1.19/+0.50	+0.37	−387
2	−1.19	+0.70/+0.54	−1.24	+0.65/+0.52	+0.66	−194	−1.27	+0.65/+0.50	+0.54	−321	−1.21	+0.65/+0.51	+0.35	−393
3	−1.20	+0.55/+0.54	−1.24	+0.49/+0.52	+0.65	−195	−1.27	+0.48/+0.50	+0.54	−321	−1.21	+0.48/+0.51	+0.34	−393
4	−1.20	+0.39/+0.54	−1.24	+0.33/+0.52	+0.63	−198	−1.27	+0.32/+0.50	+0.52	324	−1.21	+0.32/+0.51	+0.33	−397
5	−1.21	+0.54/+0.55	−1.26	+0.51/+0.52	+0.62	−208	−1.29	+0.51/+0.51	+0.51	−349	−1.23	+0.51/+0.51	+0.32	−423
6	−1.25	+1.19	−1.29	+1.16	+0.71	−179	−1.29	+1.17	+0.60	−291	−1.23	+1.18	+0.41	−358
7	−1.19	+0.69	−1.23	+0.65	+0.68	−192	−1.23	+0.63	+0.57	−298	−1.17	+0.64	+0.38	−370
8	−1.19	+0.54	−1.23	+0.49	+0.66	−194	−1.23	+0.46	+0.56	−298	−1.17	+0.46	+0.36	−370
9	−1.20	+0.38	−1.23	+0.32	+0.62	−202	−1.22	+0.29	+0.52	−305	−1.18	+0.30	+0.33	−379
10	−1.22	+0.55	−1.27	+0.51	+0.62	−217	−1.27	+0.50	+0.51	−351	−1.21	+0.50	+0.31	−427

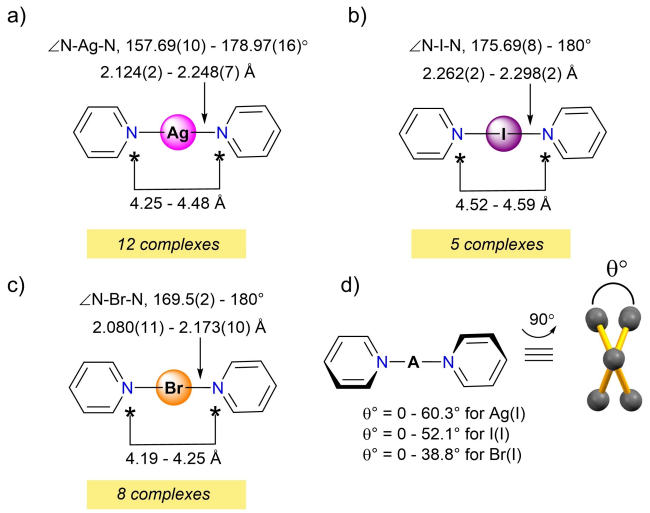

Figure 2. (a–c) Summary of XB bond parameters of crystal structures of Ag(I) and X(I) complexes, and (d) the interplanar angles (ϴ) calculated between the two pyridine ring planes. The substitution pattern and counter anions were not depicted for viewing clarity.

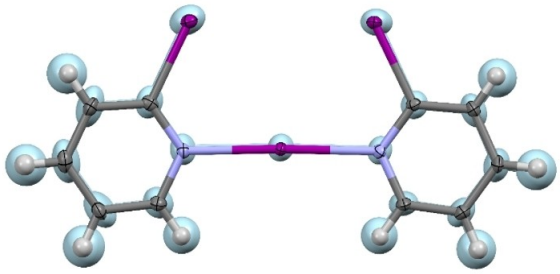

Figure 3. Overlay of the 103 K ortep plot (element colours) and the 360 K ortep plot (pale blue) for [**4**-I-**4**]PF_6.

(Figure S84). Inspired by this solid-state supramolecular receptor, we performed a temperature-dependent XRD study on [**4**-I-**4**]PF_6 between 103 and 360 K (dictated by instrument limitations) in ascending 20 K increments to probe the thermal properties and robustness of the iodine(I) (Figures 3, S85).

The [**4**-I-**4**]PF_6 was found to be thermally robust over the range of temperatures tested, with the final check at 120 K being effectively (within a 3σ error) identical to the 120 K data collected before heating to 360 K. The N–I and I–N′ bond distances (which were crystallographically independent) were found to be crystallographically indistinguishable overall temperatures tested between 103 K and 360 K (inclusive) within a 3σ tolerance (cf. 2.258(2)/2.290(2) Å at 120 K; 2.267(5)/2.299(5) Å at 360 K), which equates to a maximum increase of 0.4% in bond length. These results illustrate that the iodine(I) centre satisfies its electronic requirements to sustain linear arrangement and the [**4**-I-**4**]$^+$ framework regardless of temperature.

Computational studies

DFT calculations at the M06-2X/def-TZVP level of theory have been carried out to optimize the structures and estimate the bond energies (ΔE_{XB}) of silver(I) and halogen(I) complexes. Note the hybrid functional M06-2X is recommended for calculating XB bond energies.[27b,31] In general, the $^{+}$Ag–N bond energies for silver(I) complexes range from −179 to −217 kJ mol^{-1}, the $^{+}$I–N bond energies for iodine(I) from −291 to −351 kJ mol^{-1}, and the $^{+}$Br–N bond energies for bromine(I) from −370 to −427 kJ mol^{-1} (Table 3). The bond energies of [**L**-I-**L**]$^{+}$ are 103–134 kJ mol^{-1} larger than [**L**-Ag-**L**]$^{+}$, [**L**-Br-**L**]$^{+}$ are 176–215 kJ mol^{-1} larger than [**L**-Ag-**L**]$^{+}$, and [**L**-Br-**L**]$^{+}$ is 68–76 kJ mol^{-1} larger than [**L**-I-**L**]$^{+}$. The smallest ΔE_{XB} values are observed for fluoropyridines, and the largest for methylpyridines, indicating that the nitrogen of the fluoropyridine is weakly nucleophilic and that of methylpyridines is strongly nucleophilic. Note that the bond energies of chloro- and bromopyridines are essentially the same in 2- and 2,6-dihalopyridines-Ag(I)/X(I) complexes, with a maximum difference of 3 kJ mol^{-1} observed between [**7**-Ag-**7**]$^{+}$ and [**8**-Ag-**8**]$^{+}$.

The bond energies of 2-substituted pyridine complexes are 1-11 kJ mol^{-1} larger than those of their comparable 2,6-disubstituted pyridines for silver(I), 2-26 kJ mol^{-1} for iodine(I), and 4-29 kJ mol^{-1} for bromine(I) complexes suggesting the nitrogen of 2-substituted pyridines is more nucleophilic compared to 2,6-disubstituted pyridines. Note that the bond energies of 2-halopyridine-X(I) and analogous 2,6-dihalopyridine-X(I) complexes differ by 19-29 kJ mol^{-1} but that of 2-methylpyridine-X(I) and 2,6-dimethylpyridine-X(I) complexes do not differ more than 3.5 kJ mol^{-1} suggesting the influence of halogen substituents on the nitrogen nucleophilicity and thus on the X–N bonding is significant compared to methyl substituent. Overall, the bond energies can be ranked on substituents as follows: $CH_3 > I > Br \geq Cl > F$. The largest ΔE_{int} in iodine(I) series is for [**10**-I-**10**]$^{+}$ (−351 kJ mol^{-1}) and in bromine(I) is [**10**-Br-**10**]$^{+}$ (−427 kJ mol^{-1}).

QTAIM analysis of silver(I) and halogen(I) complexes was carried out to gain more insights into the atomic charges on nitrogen, carbons adjacent to the nitrogen, silver(I) and halogen(I) ions. The analysis showed that the positive charge transferred to pyridine rings by Br(I) of [**L**-Br-**L**]$^{+}$ complexes is 0.59 to 0.69, which is more than the positive charge transferred by I(I) in [**L**–I-**L**]$^{+}$ complexes (0.40 to 0.49) and Ag(I) in [**L**-Ag-**L**]$^{+}$ complexes (0.29 to 0.38). The magnitude of transfer depends on the nature of the substituents and hence the electron density of the pyridinic nitrogen. For instance, the I(I) of the [**1**-I-**1**]$^{+}$ transmits 0.44 positive charge to 2-fluoropyridine rings, which is less than the (I) of the [**5**-I-**5**]$^{+}$ transmitting 0.49 positive charge to 2-methylpyridine rings. The former example transfers less positive charge due to the electron-deficient 2-fluoropyridine ring, whereas the latter case transfers more positive charge due to the electron-rich 2-methylpyridine ring (see below). The atomic charge on halogen substituent bonded carbon in 2-mono and 2,6-disubstituted pyridines is more positive for larger electronegative fluorine and decreases in the order: $F > Cl > Br > I > CH_3$. Note that the trends of iodine(I) atomic charges in [**L**-I-**L**]$^{+}$ complexes are consistent with those reported for [**L**-I-**L**]$^{+}$ complexes of *para*-substituted pyridines.[27b]

We used the DFT to calculate and analyse ^{15}N NMR shifts for silver(I) and iodine(I) complexes of two representative ligands (Cl and Me) from each group (mono- and di-substituted) differing in electronic properties of their substituents. The calculations were performed at one-component scalar-relativistic (1c), and two-component spin-orbit relativistic (2c) levels of theory and the solvent environment was simulated using implicit model (dielectric constant $\varepsilon_r = 21$), Table 4. The spin-orbit (SO) coupling was expected to play more significant role for the iodine(I) assemblies comparing to their silver(I) and bromine(I) counterparts.[32] Indeed, the calculated SO shielding effect for iodine(I) systems amounts to 20–30 ppm, whereas SO deshielding for silver(I) assemblies is negligible (3-4 ppm). The calculated protonation ^{15}N NMR shifts for complexes **5** and **10** are in the typical range of about −100 ppm and correspond well with the experimental observations (Table 4). Similarly, theoretical complexation shifts for the silver(I) complexes **5** and **10** correspond well with the experimental values of about −55 ppm. Therefore, these four systems were used as benchmark. The first conclusion that can be drawn by comparing calculated and experimental data in Table 4 is inability of TFA to protonate 2-chloro and 2,6-dichloropyridine [$\Delta\delta(^{15}N_{calc})$ ~100 ppm, $\Delta\delta^{15}N_{exp}$ ~0 ppm]. The test experiments with stronger acid (HCl) resulted in a $\Delta\delta(^{15}N)$ value of −36 ppm for **2**, −80 ppm for **5**, but only −0.4 ppm for **7** and no signal observed for **10**. The X-ray crystallography of single crystals isolated from their NMR samples revealed protonated pyridinic nitrogen of **2**,[33] and **10**,[34] but not of **7** (crystallized as free pyridine, Figure S83). These results indicate that 2,6-dichloropyridinic nitrogen is less nucleophilic than that of 2-chloropyridine. The second conclusion is that the experimental coordination shifts

Table 4. Theoretical ^{15}N NMR coordination shifts [$\Delta\delta(^{15}N_{calc})$ in ppm] calculated at one-component (1c, ZORA) and two-component (2c, SO-ZORA) DFT levels of theory using ADF2022 (PBE0/TZ2P/COSMO$_{acetone}$) and experimental values.[a]

	1c	2c	Exp
[**2**-Ag-**2**]$^{+}$	−56	−52	−31
[**2**-I-**2**]$^{+}$	−57	−86	−55
[**2H**]$^{+}$	−109	−110	−2 (−36)[b]
[**5**-Ag-**5**]$^{+}$	−65	**−62**	**−53**
[**5**-I-**5**]$^{+}$	−62	−92	−102
[**5H**]$^{+}$	−124	**−124**	**−101** (−80)[b]
[**7**-Ag-**7**]$^{+}$	−44	−41	−7
[**7**-I-**7**]$^{+}$	−46	−68	−1
[**7**H]$^{+}$	−104	−105	−1 (0)[b,c]
[**10**-Ag-**10**]$^{+}$	−60	**−57**	**−50**
[**10**-I-**10**]$^{+}$	−58	−81	−90
[**10**H]$^{+}$	−124	**−124**	**−102** (–)[d]

[a]The well-correlated values used as benchmarks are highlighted in bold. [b]The values in parentheses represent $\Delta\delta(^{15}N)$ of HCl complexes. [c]The ^{15}N NMR data was collected at −20 °C since no signal were observed at −10 °C. [d]No signal observed at −10 °C and −20 °C.

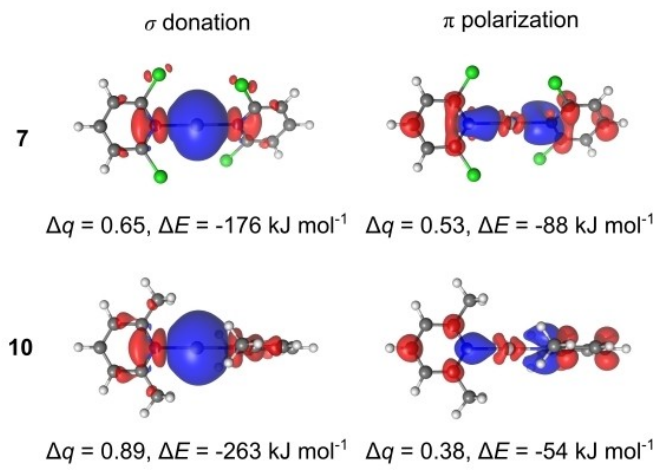

Figure 4. σ-donation (left) and π-back-donation and polarization (right) channels with the transferred charge (Δq) and orbital interaction energy (ΔE) for [**7**-Ag-**7**]$^+$ and [**10**-Ag-**10**]$^+$ constructed by summing up the most important σ and π symmetry NOCVs obtained by EDA analysis (ZORA/M06-2X/TZ2P). Regions of the charge concentration and depletion are shown in blue and red, respectively.

for silver(I) and iodine(I) assemblies of **2** amounts only about 40–60% of the predicted values and suggest fast-exchange equilibrium between the free and coordinated forms in the solution (acetone). Third, marginal experimental NMR coordination shifts for **7** indicate weak basicity of the nitrogen atom and inability of this ligand to form any stable complex is solution.

To support the indicated differences in the basicity of nitrogen atom between ligands **7** (dichloro, no complexes formed) and **10** (dimethyl, all complexes formed), we performed the energy decomposition analysis (EDA)[35] linked with Natural Orbitals for Chemical Valence (NOCV) method.[36] This approach not only allows to decompose the electron deformation density (electron rearrangement) into the various components (e.g., σ, π) of the chemical bond but it also offers to analyse the associated energy contributions to the total interaction energy. Nevertheless, the resulting NOCV channels were summed up according to their symmetry relative to the Ag–N bond and the results are shown in Figure 4. The σ-donation of nitrogen lone pair of electrons to the silver(I) ion is more pronounced for **10** with two electron-donating methyl groups and forms a stronger σ-dative bond ($\Delta E = -263$ kJ mol^{-1}). The significant difference between [**7**-Ag-**7**]$^+$ and [**10**-Ag-**10**]$^+$ in σ space is only slightly compensated for by the π-back-donation and charge polarization involving the pyridine ring (note different torsion angles). In summary, our EDA analysis supports the conclusions formulated based on the experimental and theoretical NMR data.

Conclusions

The study has demonstrated that *ortho*-functionalization of pyridines with groups of either electron-withdrawing halogens or -donating methyl results in significant changes in their solution bonding for desired halogen(I) complexes. The ^{15}N NMR coordination shifts, $\Delta\delta(^{15}N)$, i.e., the differences in the chemical shifts of pyridinic nitrogen of the complex and its respective free ligand have been related to electron-directing capabilities of substituents and their influence on nitrogen's coordination to silver(I) and halogen(I) ions. These $\Delta\delta(^{15}N)$ values are negative, generally large for 2-halo and 2-methylpyridine silver(I) and halogen(I) complexes (−21 to −102 ppm) because of the coordination-induced quenching of the paramagnetic deshielding of the non-bonding orbital at nitrogen atom (n-π^* transition). Pyridines with halogens at two *ortho*-positions to the nitrogen have drastically smaller bonding strengths, and their silver(I) and halogen(I) complexes have small $\Delta\delta(^{15}N)$ values (0 to −17 ppm) owing to electron-deficient nitrogen, indicating that they either form weak complexes or they do not complex in solution. In contrast, the large $\Delta\delta(^{15}N)$ values (−50 to −90 ppm) of silver(I) and halogen(I) complexes of 2,6-dimethylpyridine with electron-donating methyl groups reveal its strong nucleophilic nitrogen.

In crystals, *ortho*-substituents minimally affect the $^+$Ag/X–N bond distances suggesting that the magnitude of orbital overlapping between halogen(I) σ-hole and the pyridinic-N lone pair is independent of the electron density on the nitrogen altered by the *ortho*-substituents, leading to similar $^+$Ag–N and $^+$X–N bond distances. Only silver(I) complexes of 2,6-dihalopyridines and silver(I) and halogen(I) of 2,6-dimethylpyridine crystallize from their solutions. The formation of halogen(I) complexes is significantly influenced by the weak nucleophilic nitrogen of 2,6-dihalopyridines, as corroborated by the $\delta(^{15}N)$ data. Further structural analysis of silver(I) and halogen(I) complexes revealed that the pyridine rings rotate freely across the [N–Ag–N]$^+$ and [N–X–N]$^+$ bonds, with interplanar angles (ϴ) larger in silver(I) complexes (0–64.0°) than in iodine(I) (0–52.1°) and bromine(I) (0–38.3°). Although these changes in structural parameters are likely the result of crystal packing forces, the influence of the nitrogen coordination and different ligand conformations has been proposed to play a major role in halogen(I) transfer in organic synthesis.

DFT studies revealed 2-substituted pyridine complexes have larger bond energies than 2,6-disubstituted pyridine complexes. This suggests that the nitrogen of 2-substituted pyridines is more nucleophilic than that of 2,6-disubstituted pyridines, which is consistent with the ^{15}N NMR data. DFT $\Delta\delta(^{15}N)$ values of methylpyridine and chloropyridine complexes were compared to experimental $\Delta\delta(^{15}N)$. The results revealed that (i) there is a good correlation between the DFT $\Delta\delta(^{15}N)$ and experimental $\Delta\delta(^{15}N)$ for 2-methyl and 2,6-dimethylpyridine silver(I) and iodine(I) complexes, (ii) while those of 2-chloropyridine only make up roughly 40–60% of the predicted values, suggesting certain equilibrium between the free 2-chloropyridine and its coordinated forms in the solution, and (iii) the DFT $\Delta\delta(^{15}N)$ values 2,6-dichloropyridine are significantly larger than those of marginal experimental values indicating they do not form complexes in solution. Finally, the difference between 2,6-dimethyl- and 2,6-dichloro-pyridine systems was rationalized for [L–Ag–L]$^+$ complex using EDA-NOCV approach.

Experimental Section

General information

Pyridines, silver(I) salts, elemental iodine and bromine were obtained commercially (for specifics, refer to the supporting information), and they are used without purification as received. All synthesis and crystallization solvents are of HPLC grade (>99%) and are used as supplied. NMR solvents were purchased from Eurisotop. The ^{1}H and the ^{1}H-^{15}N HMBC NMR spectra were recorded on a Bruker Avance III 500 MHz instrument (For NMR spectra, see supporting information). The single-crystal X-ray data were measured using Bruker-Nonius Kappa CCD and Rigaku diffractometers and the supplementary information includes the X-ray diffractometers, data processing and structural details. The melting points were determined using BÜCHI B-540 and Stuart Scientific SMP3 apparatus. DFT calculations at the M06-2X/def-TZVP level of theory have been carried out to optimize the structures and estimate the bond energies of silver(I) and halogen(I) complexes. DFT ^{15}N NMR shifts were computed at one-component (1c, ZORA) and two-component (2c, SO-ZORA) DFT levels of theory using ADF2022 (PBE0/TZ2P/COSMO$_{acetone}$)

General synthesis of silver(I), halogen(I) and proton complexes for NMR analysis

A solution of pyridine (2.0 eq) in 0.7 mL of acetone-d_6 was mixed with silver salt (1.0 eq). The mixture was stirred to dissolve the solids. NMR was acquired. Iodine or bromine (1.1 eq) was added to the silver(I) solution, the silver(I) iodide precipitates were filtered, and NMR data were acquired for the filtrate that contained halogen(I) complex. The protonated pyridine complexes were prepared by mixing 1.0 eq of pyridine and 1.0 eq of trifluoroacetic acid in 0.7 mL of acetone-d_6, and NMR data was acquired.

General crystal synthesis of silver(I) and halogen(I) complexes for X-ray crystallography

Silver(I) salt (1.0 eq) was added to pyridine (2.0 eq) in dichloromethane (2 mL). The reaction mixture was stirred for about 3 minutes at room temperature to dissolve all solids. The clear solution was allowed to slowly evaporate to form crystals of silver(I) complexes. Solid silver(I) salts (1.0 eq) were added to pyridine (2.0 eq) dissolved in 2 mL of dichloromethane. The mixture was stirred to dissolve all the solids. Iodine or bromine (1.1 eq) was added, and light-yellow silver halide precipitates were filtered out from the solution. Evaporating the filtrate slowly produced single crystals of halogen(I) complexes that were suitable for X-ray diffraction.

Data Availability

Novotny, Jan (2023),"NMR and ETS-NOCV calculations on [Py–Ag/I–Py]$^{+}$ complexes", Mendeley Data, V1, doi: 10.17632/gcrknwv4zj.1

Crystallography data

Deposition Numbers 2302763 (for [**1**-I-**1**]PF_6), 2302764 (for [**1**-Br-**1**]PF_6), 2302765 (for [**2**-Ag-**2**]PF_6), 2302766 (for [**2**-I-**2**]Otf), 2302767 (for [**3**-Ag-**3**]PF_6), 2302768 (for [**3**-I-**3**]PF_6), 2302769 (for [**3**-Br-**3**]PF_6), 2302770 (for [**4**-Ag-**4**]PF_6), 2302771 (for [**4**-I-**4**]PF_6), 2302772 (for [**4**-Br-**4**]PF_6), 2302773 (for [**5**-Ag-**5**]PF_6), 2302774 (for [**5**-I-**5**]PF_6), 2302775 (for [**5**-I-**5**]PF_6), 2302776 (for [**5**-I-**5**]Br_3), 2302777 (for [**7**-Ag-**7**]Otf), 2302778 (for [**8**-Ag-**8**]BF_4), 2302779 (for [**9**-Ag-**9**]PF_6), 2302780 (for [**9**-Ag-**9**]Otf), 2302781 (for [**10**-Ag-**10**]PF_6), 2302782 (for [**10**-I-**10**]Otf), 2302783 (for [**10**-I-**10**]PF_6), 2302784 (for [**10**-Br-**10**]PF_6), 2302785 (for [**10**-Br-**10**]Br_3), 2302786 (for [**10**-Br-**10**]Otf), 2302787 (for [**2**-H···**2**]PF_6), 2302788 (for 7), and 2302806 (for [**8**-Ag-**8**]Otf) contain the supplementary crystallographic data for this paper. These data are provided free of charge by the joint Cambridge Crystallographic Data Centre and Fachinformationszentrum Karlsruhe Access Structures service.

Supporting Information

The Supporting Information includes information on chemicals, NMR spectra, X-ray crystallography experimental data, and DFT data. The authors have cited additional references within the Supporting Information.[37–49]

Acknowledgements

The authors gratefully acknowledge financial support from the Academy of Finland (KR grant no. 351121), and the University of Jyväskylä. The computational part of this work has received support from the Czech Science Foundation (RM grant no. 21-06991S) and MEYS CR through the e-INFRA CZ (ID:90254, JN).

Conflict of Interests

The authors declare no conflict of interest.

Data Availability Statement

The data that support the findings of this study are available from the corresponding author upon reasonable request.

Keywords: Halogen bond · coordination · halogen(I) · ortho-effect · sigma hole

[1] L. Turunen, M. Erdélyi, *Chem. Soc. Rev.* **2020**, *49*, 2688–2700.
[2] A.-C. C. Carlsson, J. Gräfenstein, J. L. Laurila, J. Bergquist, M. Erdélyi, *Chem. Commun.* **2012**, *48*, 1458–1460.
[3] Carlshon. H, Habilitationsschrift: U Ber Eine Neue Klasse von Verbindungen Des Einwertigen Jod. Verlag von S. Hirzel, Liepzig.
[4] O. Hassel, H. Hope, N. A. Sörensen, H. Dam, B. Sjöberg, J. Toft, *Acta Chem. Scand.* **1961**, *15*, 407–416.
[5] N. W. Alcock, G. B. Robertson, *Journal of the Chemical Society, Dalton Trans.* **1975**, *28*, 2483–2486.
[6] P. Pröhm, W. Berg, S. M. Rupf, C. Müller, S. Riedel, *Chem. Sci.* **2023**, *14*, 2325–2329.
[7] J. S. Ward, K.-N. Truong, M. Erdélyi, K. Rissanen, in *Comprehensive Inorganic Chemistry III*, Elsevier, Oxford, **2023**, p. 586–601.
[8] J. Barluenga, H. Vázquez-Villa, A. Ballesteros, J. M. González, *J. Am. Chem. Soc.* **2003**, *125*, 9028–9029.
[9] a) J. Barluenga, J. M. González, P. J. Campos, G. Asensio, *Angew. Chem. Int. Ed.* **1985**, *24*, 319–320; b) J. Barluenga, *Pure Appl. Chem.* **1999**, *71*, 431–436.
[10] J. Barluenga, F. González-Bobes, M. C. Murguía, S. R. Ananthoju, J. M. González, *Chem. Eur. J.* **2004**, *10*, 4206–4213.
[11] a) A.-C. C. C. Carlsson, J. Gräfenstein, A. Budnjo, J. L. Laurila, J. Bergquist, A. Karim, R. Kleinmaier, U. Brath, M. Erdélyi, *J. Am. Chem. Soc.* **2012**, *134*,

5706–5715; b) J. S. Ward, A. Frontera, K. Rissanen, *Dalton Trans.* **2021**, *50*, 8297–8301; c) J. S. Ward, R. M. Gomila, A. Frontera, K. Rissanen, *RSC Adv.* **2022**, *12*, 8674–8682.
[12] a) S. Lindblad, K. Mehmeti, A. X. Veiga, B. Nekoueishahraki, J. Gräfenstein, M. Erdélyi, *J. Am. Chem. Soc.* **2018**, *140*, 13503–13513; b) S. Yu, J. S. Ward, *Dalton Trans.* **2022**, *51*, 4668–4674.
[13] G. R. Desiraju, P. Shing Ho, L. Kloo, A. C. Legon, R. Marquardt, P. Metrangolo, P. Politzer, G. Resnati, K. Rissanen, *Pure Appl. Chem.* **2013**, *85*, 1711–1713.
[14] E. Arunan, G. R. Desiraju, R. A. Klein, J. Sadlej, S. Scheiner, I. Alkorta, D. C. Clary, R. H. Crabtree, J. J. Dannenber, P. Hobza, H. G. Kjaergaard, A. C. Legon, B. Mennucci, D. J. Nesbitt, *Pure Appl. Chem.* **2011**, *83*, 1637–1641.
[15] P. L. Bora, M. Novák, J. Novotný, C. Foroutan-Nejad, R. Marek, *Chem. Eur. J.* **2017**, *23*, 7315–7323.
[16] a) L. Turunen, U. Warzok, C. A. Schalley, K. Rissanen, *Chem* **2017**, *3*, 861–869; b) L. Turunen, A. Peuronen, S. Forsblom, E. Kalenius, M. Lahtinen, K. Rissanen, *Chem. Eur. J.* **2017**, *23*, 11714–11718; c) L. Turunen, U. Warzok, R. Puttreddy, N. K. Beyeh, C. A. Schalley, K. Rissanen, *Angew. Chem. Int. Ed.* **2016**, *55*, 14033–14036; d) E. Taipale, J. S. Ward, G. Fiorini, D. L. Stares, C. A. Schalley, K. Rissanen, *Inorg. Chem. Front.* **2022**, *9*, 2231–2239.
[17] A. Vanderkooy, A. K. Gupta, T. Földes, S. Lindblad, A. Orthaber, I. Pápai, M. Erdélyi, *Angew. Chem. Int. Ed.* **2019**, *58*, 9012–9016.
[18] G. Gong, S. Lv, J. Han, F. Xie, Q. Li, N. Xia, W. Zeng, Y. Chen, L. Wang, J. Wang, S. Chen, *Angew. Chem. Int. Ed.* **2021**, *60*, 14831–14835.
[19] a) A.-C. C. Carlsson, M. Uhrbom, A. Karim, U. Brath, J. Grafenstein, M. Erdelyi, *CrystEngComm* **2013**, *15*, 3087–3092; b) M. Bedin, A. Karim, M. Reitti, A.-C. C. Carlsson, F. Topic, M. Cetina, F. Pan, V. Havel, F. Al-Ameri, V. Sindelar, K. Rissanen, J. Grafenstein, M. Erdelyi, *Chem. Sci.* **2015**, *6*, 3746–3756.
[20] a) J. S. Ward, A. Frontera, K. Rissanen, *Inorg. Chem.* **2021**, *60*, 5383–5390; b) S. Yu, P. Kumar, J. S. Ward, A. Frontera, K. Rissanen, *Chem* **2021**, *7*, 948–958; c) S. Wilcox, D. Sethio, J. S. Ward, A. Frontera, R. Lindh, K. Rissanen, M. Erdélyi, *Chem. Commun.* **2022**, *58*, 4977–4980.
[21] D. Von der Heiden, K. Rissanen, M. Erdélyi, *Chem. Commun.* **2020**, *56*, 14431–14434.
[22] K. Rissanen, M. Haukka, in *Halogen Bonding II SE - 587* (Eds.: P. Metrangolo, G. Resnati), Springer International Publishing, Switzerland, **2015**, p. 77–90.
[23] T. Okitsu, S. Yumitate, K. Sato, Y. In, A. Wada, *Chem. Eur. J.* **2013**, *19*, 4992–4996.
[24] B. Simonot, G. Rousseau, *J. Org. Chem.* **1994**, *59*, 5912–5919.
[25] a) R. Marek, in *Encyclopedia of Spectroscopy and Spectrometry (Third Edition)* (Eds.: J. C. Lindon, G. E. Tranter, D. W. Koppenaal), Academic Press, Oxford, **2017**, p. 110–116; b) R. Marek, A. Lycka, *Curr Org Chem* **2002**, *6*, 35–66.
[26] L. Pazderski, *Magn. Reson. Chem.* **2008**, *46*, S3–S15.
[27] a) R. Kleinmaier, S. Arenz, A. Karim, A.-C. C. Carlsson, M. Erdélyi, *Magn. Reson. Chem.* **2013**, *51*, 46–53; b) D. Sethio, G. Raggi, R. Lindh, M. Erdélyi, *J. Chem. Theory Comput.* **2020**, *16*, 7690–7701.
[28] S. B. Hakkert, M. Erdélyi, *J. Phys. Org. Chem.* **2015**, *28*, 226–233.
[29] L. Yang, D. R. Powell, R. P. Houser, *Dalton Trans.* **2007**, 955–964.
[30] T. Bunchuay, A. Docker, A. J. Martinez-Martinez, P. D. Beer, *Angew. Chem. Int. Ed.* **2019**, *131*, 13961–13965.
[31] M. Novák, C. Foroutan-Nejad, R. Marek, *Phys. Chem. Chem. Phys.* **2015**, *17*, 6440–6450.
[32] J. Vicha, J. Novotny, S. Komorovsky, M. Straka, M. Kaupp, R. Marek, *Chem. Rev.* **2020**, *120*, 7065–7103.
[33] M. Frey, P. G. Jones, *Z. Naturforsch. B* **2001**, *56*, 889–896.
[34] Effendy, P. C. Junk, C. J. Kepert, L. M. Louis, T. C. Morien, B. W. Skelton, A. H. White, *Z. Anorg. Allg. Chem.* **2006**, *632*, 1312–1325.
[35] F. M. Bickelhaupt, E. J. Baerends, *Rev. Comput. Chem.*, John Wiley & Sons Ltd, New Jersey, **2000**, p. 1–86.
[36] M. P. Mitoraj, A. Michalak, T. Ziegler, *J. Chem. Theory Comput.* **2009**, *5*, 962–975.

Manuscript received: November 2, 2023
Accepted manuscript online: December 6, 2023
Version of record online: January 15, 2024